

Ocean Color Continuity From VIIRS Measurements Over Tampa Bay

Chuanmin Hu and Chengfeng Le

Abstract—Ocean color continuity calls for consistent observations from multiple sensors in order to establish a seamless data record to address earth science questions. Currently, both Moderate Resolution Imaging Spectroradiometer (MODIS) instruments on the Terra and Aqua satellites are being operated well beyond their designed five-year mission life, and they have shown signs of sensor degradation. It is thus urgent to evaluate whether the most recently launched Visible Infrared Imager Radiometer Suite (VIIRS) instrument (2011 to present) can provide consistent observations should MODIS instruments stop functioning. In this study, the consistency between MODIS/Aqua and VIIRS measurements over the Tampa Bay estuary ($\sim 1000 \text{ km}^2$) is assessed for remote sensing reflectance (R_{rs} , sr^{-1}), chlorophyll-*a* concentrations (Chla , $\text{mg} \cdot \text{m}^{-3}$), and absorption coefficient of colored dissolved organic matter ($a_g(443)$, m^{-1}). While R_{rs} was derived as a standard National Aeronautics and Space Administration product from the SeaDAS software package (reprocessing version R2013.0), Chla and $a_g(443)$ were estimated using the recently developed regional algorithms for Tampa Bay. Time-series analysis and statistics both showed that the two sensors provided consistent measurements for most products evaluated, with unbiased mean percentage differences of $< 25\%$ and mean annual biases within -9% (except for one of the eight cases) for large dynamic ranges in Chla ($1.0\text{--}20 \text{ mg} \cdot \text{m}^{-3}$) and $a_g(443)$ ($0.1\text{--}1.5 \text{ m}^{-1}$) in all four bay segments. These estimates are comparable or better than those derived from satellite—*in situ* comparisons, suggesting that VIIRS will provide observations consistent with MODIS, ensuring ocean color continuity and seamless data records for Tampa Bay. Such observations are crucial in establishing a long-term satellite-based water quality decision matrix for Tampa Bay.

Index Terms—Continuity, Moderate Resolution Imaging Spectroradiometer (MODIS), Sea-viewing Wide Field-of-view Sensor (SeaWiFS), Tampa Bay, Visible Infrared Imager Radiometer Suite (VIIRS), water quality.

I. INTRODUCTION

ONE of the primary goals of launching ocean color satellites is to obtain long-term, synoptic, and reliable measurements of ocean properties to address critical earth science questions. The time scale required to address these questions often ranges from years to decades. On the other hand, ocean color missions are typically designed to have a five-

year mission life. To overcome this problem, it is necessary to use multiple sensors to form a multidecadal data record. However, achieving such a goal is by no means trivial and requires substantial effort in sensor calibration, algorithm development, and data product validation.

Global and regional validation has shown that, if uncertainties in the field-measured data were removed, uncertainties in the satellite-derived remote sensing reflectance (R_{rs} , sr^{-1}) in the blue bands would reach a few percent for blue waters [1], [2], [4], [14], [21], [25], meeting the 5% mission requirement [12]. Chlorophyll-*a* concentration (Chla , $\text{mg} \cdot \text{m}^{-3}$) estimated from the satellite-derived R_{rs} has often shown root-mean-square differences from field-measured Chla of $0.2\text{--}0.3$ (after logarithmic transformation) without significant bias [2], [10], [20], [26]. More recently, [7] have shown that mean R_{rs} over the global ocean from the Sea-viewing Wide Field-of-view Sensor (SeaWiFS, 1997–2010) and the Moderate Resolution Imaging Spectroradiometer (MODIS) on Aqua (2002 to present) agreed with each other to within a few percent for most spectral bands. Considering that the ocean signal is often $< 10\%$ of the satellite signal, this is a marvelous achievement.

This accomplishment is attributed to the continuous improvement in calibration, processing algorithms, and correction of sensor artifacts (e.g., out-of-band response, temporal degradation, etc.). To ensure cross-sensor consistency, it is critical to have two sensors operating at the same time (e.g., SeaWiFS and MODIS). Even so, periodic reprocessing is required to incorporate the most recent advances in calibration updates and algorithm development. For example, ocean color data from several sensors have been reprocessed 12 times since 1998 by the NASA Ocean Biology Processing Group (OBPG) (<http://oceancolor.gsfc.nasa.gov/WIKI/OCReproc.html>).

The Visible Infrared Imager Radiometer Suite (VIIRS) instrument on the Suomi National Polar-orbiting Partnership satellite was launched in October 2011, after which the data have been operationally processed by the NOAA Interface Data Processing System (IDPS) and reprocessed by the NASA OBPG. Global products of spectral R_{rs} and Chla showed reasonable agreement with concurrent MODIS from both the IDPS processing [24] and the OBPG processing [8]. However, it is unclear whether VIIRS data products in turbid estuaries are consistent with the corresponding MODIS products. On the other hand, recent advances in algorithm development have led to reliable data products for some estuaries, making it possible to establish long-term data records to evaluate the estuarine water quality state (e.g., [15] and [16]). Thus, given the fact that MODIS is aging (12 years old at the time of this writing), whereas VIIRS is relatively new, it is urgent to evaluate whether VIIRS can provide continuity for estuarine water quality monitoring, when the MODIS era ends.

Manuscript received July 17, 2013; revised August 22, 2013; accepted September 15, 2013. Date of publication October 22, 2013; date of current version December 11, 2013. This work was supported by the National Aeronautics and Space Administration's Water and Energy, Ocean Biology and Biogeochemistry, and Gulf of Mexico Programs.

The authors are with the College of Marine Science, University of South Florida, St. Petersburg, FL 33701 USA (e-mail: huc@usf.edu).

Color versions of one or more of the figures in this paper are available online at <http://ieeexplore.ieee.org>.

Digital Object Identifier 10.1109/LGRS.2013.2282599

To achieve this objective, we selected Tampa Bay as a test case for three reasons: First, Tampa Bay is a typical estuary with complex optical properties, where both colored dissolved organic matter (CDOM) and nonliving particles significantly contribute to total absorption coefficients and Rrs [17]. With a surface area of $\sim 1000 \text{ km}^2$ and an average water depth of 4 m, all optical constituents can substantially vary in both space and time [17]; turbidity ranges from 1 to 10 nephelometric turbidity units, Chla from 1.0 to 100 $\text{mg} \cdot \text{m}^{-3}$, and CDOM absorption coefficient at 443 nm ($a_g(443)$) from 0.1 to 8 m^{-1} . Second, a significant amount of effort has been dedicated to establish a water quality decision matrix (WQDM) from both field measurements [9] and satellite observations [16]. The WQDM was established from water quality data based on predefined threshold values for each bay segment; exceeding the thresholds would call for either attention or management actions. Finally, regional algorithms have been developed and validated to derive Chla and $a_g(443)$ [16], [18]. The choice of Tampa Bay, as a typical estuary, is well suited for the evaluation of VIIRS continuity for these well-established data products.

II. DATA AND METHOD

VIIRS and MODIS Level-2 data (from January 1 to December 31, 2012) containing the spectral Rrs and quality control flags (l2_flags) at 1-km and 750-m resolutions, respectively, were obtained from the NASA Goddard Space Flight Center at the end of February 2013. These data were generated by the NASA OBP using the most recent updates in calibration and sensor artifacts correction (reprocessing version R2013.0; <http://oceancolor.gsfc.nasa.gov/WIKI/OCReproc.html>). Briefly, an on-orbit vicarious calibration [6] and a NIR iterative atmospheric correction algorithm [3] were applied to process all data. The bidirectional reflectance distribution function (BRDF) effect was corrected following the approach of [22].

The daily Rrs(λ) data were used to derive Chla using a red-green-chlorophyll-index (RGCI) algorithm [16], i.e.,

$$\text{Chla} = 0.85 \times \exp(5.1 \times \text{RGCI}), \text{RGCI} = \text{Rrs667}/\text{Rrs547}. \quad (1)$$

$a_g(443)$ was derived from the satellite-retrieved Rrs(λ) using a hybrid approach to combine the advantages of semianalytical and empirical algorithms [18]. The approach first used a modified quasi-analytical algorithm [19] to estimate the total absorption, i.e., a_t , and then subtracted empirically estimated phytoplankton and nonalgal particle absorptions from a_t . Both algorithms were specifically designed for Tampa Bay for its specific optical properties, and they achieved $\sim 30\%$ uncertainties for both Chla and $a_g(443)$ for large dynamic ranges. The resulting data—Rrs(λ), Chla, $a_g(443)$, and l2_flags—were all mapped to a rectangular projection over Tampa Bay. The daily maps were used to compose monthly maps, where data associated with the following quality control flags were excluded: ATMFAIL (1), LAND (2), HIGLINT(4), HILT (5), HISATZEN (6), STRAYLIGHT (9), CLDICE (10), COCCOLITH (11), HISOLZEN (13), LOWLW (15), CHLFAIL (16), NAVWARN (17), MAXAERITER (20), CHLWARN (22), ATMWARN (23), NAVFAIL (26), and FILTER (27). The numbers in the parentheses represent the bit position of the 32-bit flag value.

To minimize possible interference from the shallow bottom, satellite pixels with bottom depths of $< 2 \text{ m}$ were excluded [5]. For point comparisons, a spatial homogeneity test using a 3×3 pixel window was used to further screen the data [11].

Two methods of data comparison were used. The first focused on a single station (27.66° N , 82.59° W) in the middle Tampa Bay (MTB) to examine how data from individual pixel locations agree with, or differ from, each other. This is Station #23 from a monthly survey program of the Environmental Protection Commission of Hillsborough County (EPCHC), where satellite match-up data have been reported earlier [16], [18]. The rigorous quality control criteria resulted in 72 matching pairs between MODIS and VIIRS for 2012. In the second method, each of the 4 bay segments was treated as a whole to establish time series data. Several measures were used to perform the statistical analysis. The first was the coefficient of determination, i.e., R^2 , followed by an unbiased percentage difference (UPD) defined as [13]

$$\text{UPD}(\%) = 1/N \sum [0.5(y_i - x_i)/(y_i + x_i)] \times 100 \quad (2)$$

where N is the number of data pairs, the subscript i stands for the individual data point, and x and y represent the two variables being evaluated (in this case, VIIRS- and MODIS-derived water properties). The reason to use the unbiased form of $[0.5(y_i - x_i)/(y_i + x_i)]$ instead of the normal form of $[(y_i - x_i)/x_i]$ is because both data sets may contain substantial errors in both directions (positive and negative). If x_i is significantly biased low, the ratio of $[(y_i - x_i)/x_i]$ may become extremely large, leading to unrealistic estimates of percentage difference. The use of $[0.5(y_i - x_i)/(y_i + x_i)]$ avoids this problem. Finally, the mean relative difference (MRD) was used as a measure of the mean bias between the two data sets

$$\text{MRD}(\%) = 1/N \sum [(y_i - x_i)/x_i] \times 100. \quad (3)$$

III. RESULTS

Fig. 1 compares Rrs(λ) daily time series of MODIS and VIIRS for the MTB station in Tampa Bay (27.66° N , 82.59° W), whereas the scatter plots are shown in Fig. 2, and statistics are summarized in Table I. Consistent temporal patterns can be visualized between MODIS and VIIRS Rrs for all wavelengths evaluated, with the 551-nm band showing the best consistency and the 443-nm band the worst. The statistical measures also showed the same results, which are consistent with those from the MODIS—*in situ* Rrs comparison, where the 443-nm band showed the highest degree of uncertainty of $\sim 45\%$, as compared with the $\sim 20\%$ uncertainties for Rrs at 547 and 667 nm [15]. The cross-sensor difference is comparable with these *in situ*-based uncertainty estimates. Note that the relative Rrs differences appear larger for small Rrs(547) and Rrs(667) ranges in the log-log plots in Fig. 2(a) and (d), but the absolute differences are less insensitive to the data ranges.

While Figs. 1 and 2 show data comparison solely at one location, Fig. 3 represents the spatial distributions of Rrs difference between MODIS and VIIRS. There is a distinctive spatial pattern for 443 and 486 nm, where the upper bay segments showed higher UPD than the lower bay segments. The UPD at 443 nm is generally $> 50\%$ for all bay segments, except

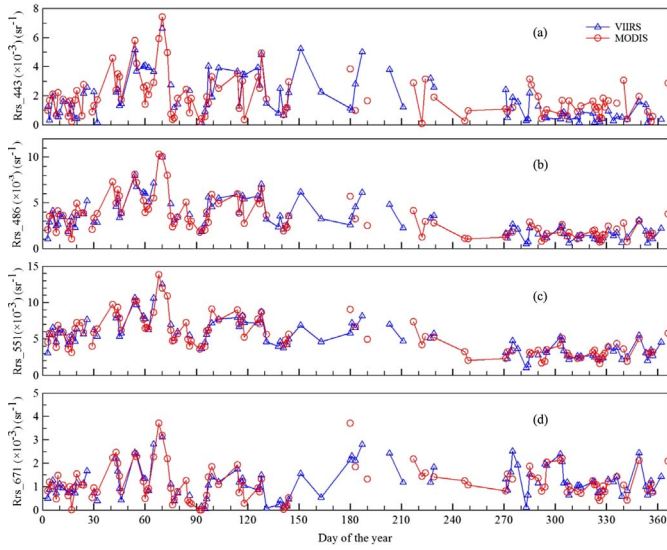


Fig. 1. Comparison of $Rrs(\lambda)$ of MODIS and VIIRS in 2012 for the MTB station in Tampa Bay (27.66° N, 82.59° W).

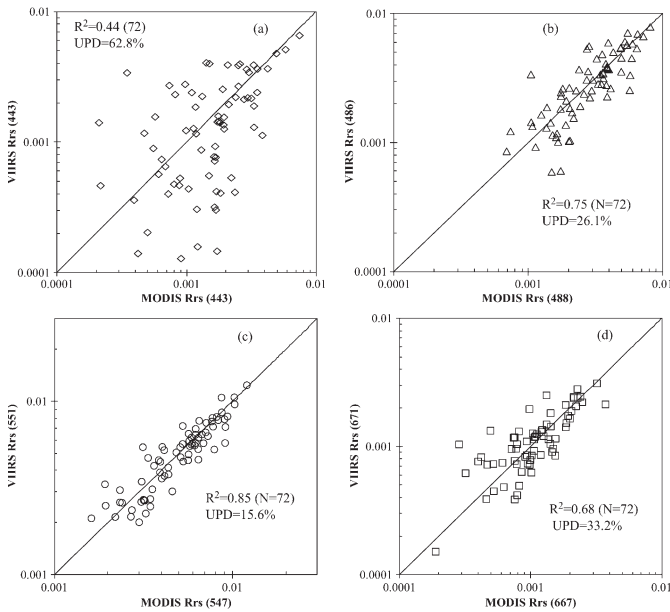


Fig. 2. Same as Fig. 1 but data are presented in scatter plots when both VIIRS and MODIS had valid measurements on the same day. The UPD is also presented in the figures and summarized in Table I.

TABLE I
COMPARISON OF VIIRS AND MODIS RRS DATA AT THE MTB STATION
IN TAMPA BAY ($N = 72$ FOR DAILY DATA OF 2012)

	Rrs443	Rrs486	Rrs551	Rrs671	Chla	$a_g(443)$
R^2	0.44	0.75	0.85	0.68	0.86	0.76
MRD	-20.9%	-4.3%	-0.9%	-16.9%	-12.4%	3.0%
UPD	62.8%	26.1%	15.6%	33.2%	21.1%	33.4%

the Lower Tampa Bay (LTB). The UPD at 486 nm is between 30% and 40% for Old Tampa Bay (OTB) and Hillsborough Bay (HB), but significantly lower ($< 20\%$) for the MTB and the LTB. The UPD at 551 nm is $< 20\%$ and the UPD at 671 nm is $< 30\%$ for nearly all bay waters. More importantly, there is no systematic spatial pattern at 551 and 671 nm.

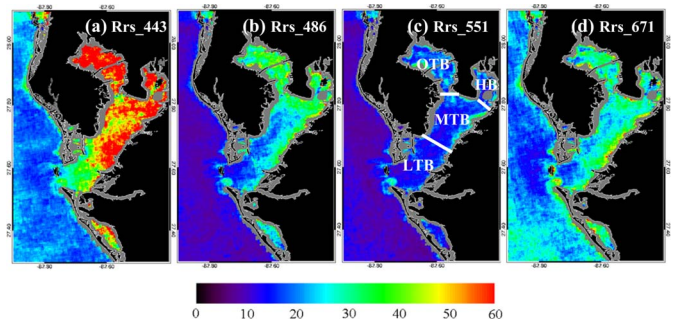


Fig. 3. Spatial distribution of annual mean UPD (%) between MODIS and VIIRS daily Rrs for the year 2012. In (c), the locations of the four bay segments are annotated: Old Tampa Bay, Hillsborough Bay, Middle Tampa Bay, and Lower Tampa Bay.

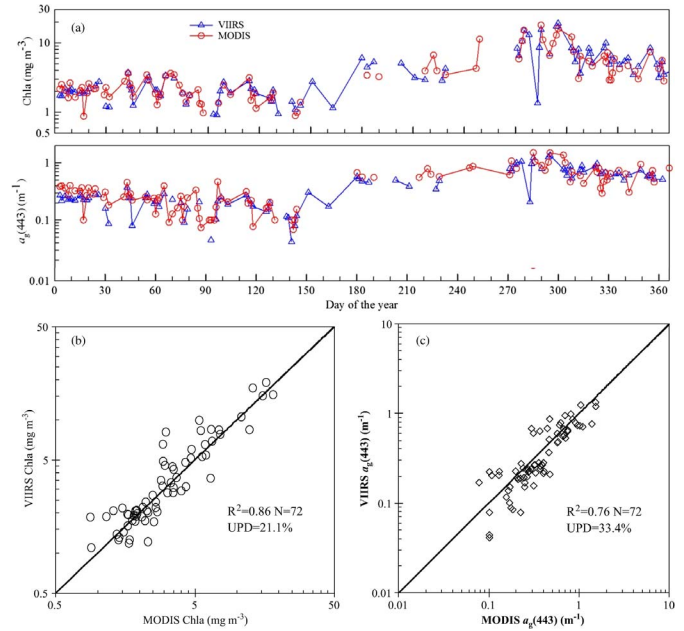


Fig. 4. Comparison of $Chla$ and $a_g(443)$ derived from MODIS and VIIRS measurements in 2012 at the MTB station in Tampa Bay (27.66° N, 82.59° W). The statistical measures are summarized in Table I.

These results have significant implications on biooptical algorithms relying on green and red wavelengths, as these bands showed the best cross-sensor consistency and almost uniform spatial UPD patterns. Indeed, Fig. 4 shows excellent agreement between MODIS and VIIRS estimates of $Chla$ and $a_g(443)$ in both the temporal patterns and statistical measures when these products are estimated with the algorithms relying on the green and red bands [16], [18]. The UPD for $Chla$ is 21.1% and the UPD for $a_g(443)$ is 33.4% for large dynamic ranges in $Chla$ (about $1\text{--}20\text{ mg}\cdot\text{m}^{-3}$) and $a_g(443)$ (about $0.1\text{--}1.5\text{ m}^{-1}$). In comparison, the mean relative error (MRE, unsigned) of the MODIS-derived $Chla$ was 25.8% with a R^2 of 0.83 ($1\text{--}30\text{ mg}\cdot\text{m}^{-3}$, $N = 38$) when similar field-measured $Chla$ [15, Fig. 3] was used to gauge the MODIS performance. The MRE of the MODIS-derived $a_g(443)$ was 23.7% with a R^2 of 0.72 ($0.3\text{--}8\text{ m}^{-1}$, $N = 33$) when field-measured $a_g(443)$ was used to gauge MODIS performance [18]. There is no apparent spatial pattern in the annual mean UPD between data products of the two sensors (see Fig. 5), suggesting that MODIS and VIIRS $Chla$ and $a_g(443)$ may be interchangeably used for most locations when annual statistics are used to evaluate water quality status.

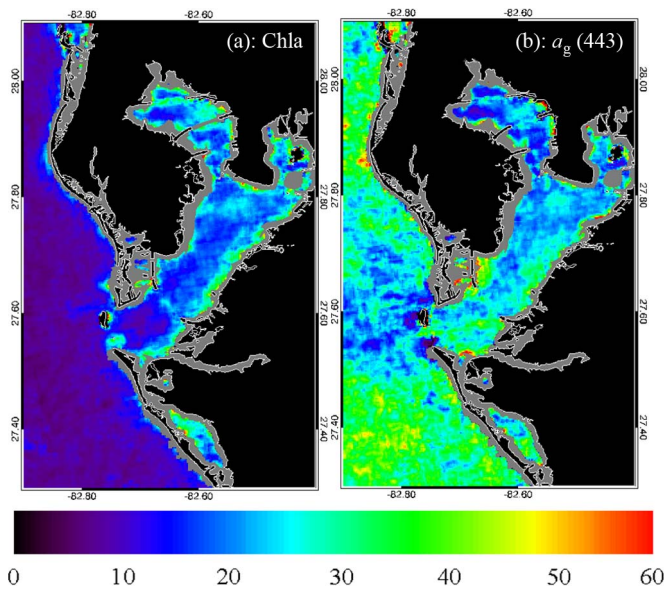


Fig. 5. Spatial distribution of annual mean UPD (%) between MODIS- and VIIRS-derived Chla and $a_g(443)$ using the RGCI algorithm [16] and the hybrid approach [18], respectively.

Fig. 6 further shows excellent consistency between the two products for all bay segments when each segment was treated as a whole, with UPD always < 25% and MRD within -9% (except for one of the eight cases). This result is better than the 35% mission goal for the Chla retrieval accuracy [12], suggesting satisfactory performance of VIIRS in continuing observations from the MODIS era.

IV. DISCUSSION

As expected, for the four bands evaluated, $R_{rs}(443)$ showed the worst consistency between the two sensors. Similar results from *in situ* validations have been reported earlier. Although not shown, the performance of $R_{rs}(412)$ is even worse. This is apparently due to problems in the atmospheric correction, which extrapolates aerosol properties from the NIR to the visible. This effect has been shown in a recent paper to evaluate R_{rs} uncertainties (in both their absolute magnitudes and relative units) based on satellite measurements alone [14]. Tampa Bay is rich in both phytoplankton and CDOM, leading to high absorption and low R_{rs} in the blue [17]. Then, the same R_{rs} uncertainties would lead to much higher relative errors for low- $R_{rs}(443)$ waters, as demonstrated in Fig. 2(a). The same effect can also explain the uneven UPD distributions in $R_{rs}(443)$ [see Fig. 3(a)] and $R_{rs}(486)$ [see Fig. 3(b)], because the upper bay segments have higher concentrations of phytoplankton and CDOM than in the LTB, leading to higher blue-light absorption, lower $R_{rs}(443)$, and higher UPD [see Fig. 2(a)].

VIIRS and MODIS may view the same location at different angles on the same day, and there are also slight differences between their bandwidths and band centers (e.g., 547 nm for MODIS and 551 nm for VIIRS). Most of these differences are removed (or at least minimized) by the atmospheric correction and the BRDF correction specifically designed for each sensor. The quality control during data screening excluded data with extremely large viewing angles ($> 60^\circ$). However, there might be residual BRDF correction errors that contributed to the data

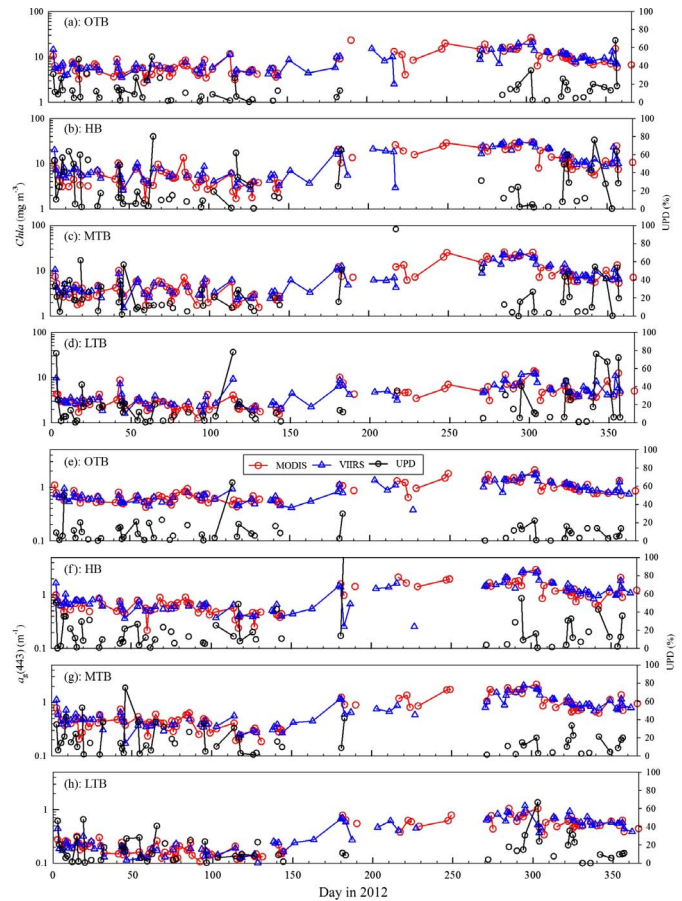


Fig. 6. Daily mean Chla and $a_g(443)$ of the four bay segments derived from MODIS and VIIRS measurements. The x -axis shows the day of the year in 2012 (1–366). In addition, shown in the figures are the UPDs for each data pair (x -axis on the right). For Chla, the mean UPD is 15.0%, 25.3%, 22.1%, and 17.6% for the four bay segments (OTB, HB, MTB, and LTB), respectively; and the MRD is -3.7% , -21.3% , -5.4% , and -9.1% for the four bay segments, respectively ($N = 59$). For $a_g(443)$, the mean UPD is 10.6%, 18.1%, 17.0%, and 14.6% for the four bay segments, respectively; and the MRD is -2.3% , -7.6% , -1.0% , and -0.5% for the four bay segments, respectively ($N = 59$).

scatter in Fig. 2(a), which require more in-depth analysis that is beyond the scope of this work.

The evaluation results have significant implications for long-term water quality monitoring and management in Tampa Bay. First, VIIRS can continue the MODIS observations with comparable data quality to extend the water quality data records in the coming years. Second, it demonstrates that, even with a relatively short mission life (designed for five years), it is possible to remove the sensor-specific differences (sensor design and observing geometry) to obtain consistent data records for coastal waters. Finally, while modern satellite observations of estuarine water quality did not start until the late 1990s, it is possible to form a multidecadal data record using multiple satellite missions. This is particularly useful for observing decadal changes of water quality in response to large-scale climate variability, such as the El Niño–Southern Oscillation and the Atlantic Multidecadal Oscillation (e.g., [16]). The multisensor consistency is also a critical requirement for establishing numeric nutrient criteria in order to maintain a healthy coastal ecosystem [23].

Can these observations be extended to other estuaries or coastal waters? Evaluation results for a clear-water site in the Gulf of Mexico (26.0° N, -88.0° E) are similar to those presented here, i.e., consistent performance for the green and

red bands but worse performance for the blue bands. If the blue bands are used in the inversion algorithms such as in the standard blue–green band ratio Chla algorithm, large inconsistencies will result in the data products. If the algorithms avoid the blue bands such as those used for Tampa Bay Chla and $a_g(443)$, product consistency will be improved. However, this is based on the assessment under relatively clear atmospheres (e.g., mean aerosol optical thickness at 865 nm and $\tau_a(865)$ is about 0.08 for the Gulf of Mexico). For estuaries under more turbid atmospheres (e.g., mean $\tau_a(865) \sim 0.16$ for the East China Sea), the consistency may become much worse due to increased uncertainties in the atmospheric correction. In any case, it is wise to perform a similar consistency assessment for any particular estuary of interest.

The results presented here are based on data products generated by the NASA OBPG, as these products and their associated processing software (SeaDAS) have been widely available to and used by the community. We recognize that independent to the NASA processing, NOAA has initialized the operational IDPS processing. The consistency between the operational IDPS VIIRS products and the MODIS products will be evaluated in a follow-on work in order to maximize the potentials of these operational products. Likewise, the impact of the lack of VIIRS fluorescence bands on bloom detection and quantification in optically complex waters will also be evaluated.

V. CONCLUSION

Multidecadal and synoptic assessments of estuarine water quality can only be achieved through combining multisensor observations, where cross-sensor consistency is a key requirement to assure data continuity. Comparison between MODIS (Aqua) and VIIRS data products for the period of 2012 over Tampa Bay indicated satisfactory consistency in the Rrs (green and red bands), Chla, and CDOM products, where the difference between sensors is comparable or less than the product uncertainty when gauged by field measurements. The results demonstrate that, despite the difference between the sensor characteristics and the observing geometry, it is possible to establish multisensor data records to assess estuarine water quality in a consistent manner.

ACKNOWLEDGMENT

The authors would like to thank the NASA OBPG for providing all satellite data and processing software and two anonymous reviewers for their extensive comments.

REFERENCES

- [1] D. Antoine, F. d'Ortenzio, S. B. Hooker, G. Bécu, B. Gentili, D. Tailliez, and A. J. Scott, "Assessment of uncertainty in the ocean reflectance determined by three satellite ocean color sensors (MERIS, SeaWiFS and MODIS-A) at an offshore site in the Mediterranean Sea (BOUSSOLE project)," *J. Geophys. Res.*, vol. 113, no. C7, pp. C07013–1–C07013–22, Jul. 2008.
- [2] S. W. Bailey and P. J. Werdell, "A multi-sensor approach for the on-orbit validation of ocean color satellite data products," *Remote Sens. Environ.*, vol. 102, no. 1/2, pp. 12–23, May 2006.
- [3] S. W. Bailey, B. A. Franz, and P. J. Werdell, "Estimation of near-infrared water-leaving reflectance for satellite ocean color data processing," *Opt. Exp.*, vol. 18, no. 17, pp. 7521–7527, Mar. 2010.
- [4] J. P. Cannizzaro, C. Hu, K. L. Carder, C. R. Kelble, N. Melo, E. M. Johns, G. A. Vargo, and C. A. Heil, "On the accuracy of SeaWiFS ocean color data products on the West Florida Shelf," *J. Coastal Res.*, to be published.
- [5] Z. Chen, F. E. Muller-Karger, and C. Hu, "Remote sensing of water clarity in Tampa Bay," *Remote Sens. Environ.*, vol. 109, no. 2, pp. 249–259, Jul. 2007.
- [6] R. Eplee, K. R. Turpie, G. F. Fireman, G. Meister, T. C. Stone, F. S. Patt, B. A. Franz, S. W. Bailey, and C. R. McClain, "VIIRS on-orbit calibration for ocean color data processing observing systems," in *Proc. SPIE 8510, Earth Obs. Syst. XVII*, Oct. 2012, p. 85101G.
- [7] B. A. Franz, S. W. Bailey, G. Meister, and P. J. Werdell, "Quality and consistency of the NASA ocean color data record," in *Proc. Ocean Opt. XXI*, Glasgow, U.K., Oct. 8–12, 2012.
- [8] B. A. Franz, "NASA satellite ocean color time series," in *Proc. Int. Ocean Color Sci. Meet.*, Darmstadt, Germany, May 6–8, 2013, pp. 1–57.
- [9] H. Greening and A. Janicki, "Toward reversal of eutrophic conditions in a subtropical estuary: Water quality and seagrass response to nitrogen loading reductions in Tampa Bay, Florida, USA," *Environ. Manage.*, vol. 38, no. 2, pp. 163–178, Aug. 2006.
- [10] W. W. Gregg and N. W. Casey, "Global and regional evaluation of the SeaWiFS chlorophyll data set," *Remote Sens. Environ.*, vol. 93, pp. 463–479, 2004.
- [11] L. W. Harding, Jr., A. Magnuson, and M. E. Mallonee, "SeaWiFS retrievals of chlorophyll in Chesapeake Bay and the mid-Atlantic bight," *Estuarine, Coastal Shelf Sci.*, vol. 62, no. 1/2, pp. 75–94, Jan. 2005.
- [12] S. B. Hooker, W. E. Esaias, G. C. Feldman, W. W. Gregg, and C. R. McClain, "An overview of SeaWiFS and ocean color," Natl. Aeronautics Space Admin., Goddard Space Flight Center, Greenbelt, MD, USA, NASA Tech. Memo. 104566, 1992.
- [13] S. B. Hooker, G. Lazin, G. Zibordi, and S. McLean, "An evaluation of above- and in-water methods for determining water-leaving radiances," *J. Atmos. Ocean. Technol.*, vol. 19, no. 4, pp. 486–515, Apr. 2002.
- [14] C. Hu, L. Feng, and Z. Lee, "Uncertainties of SeaWiFS and MODIS remote sensing reflectance: Implications from clear water measurements," *Remote Sens. Environ.*, vol. 133, pp. 163–182, Jun. 2013.
- [15] C. Le, C. Hu, D. English, J. Cannizzaro, Z. Chen, L. Feng, R. Boler, and C. Kovach, "Towards a long-term chlorophyll-a data record in a turbid estuary using MODIS observations," *Progr. Oceanogr.*, vol. 109, pp. 90–103, Feb. 2013.
- [16] C. Le, C. Hu, J. Cannizzaro, D. English, and C. Kovach, "Climate-driven chlorophyll a changes in a turbid estuary: Observation from satellites and implications for management," *Remote Sens. Environ.*, vol. 130, pp. 11–24, Mar. 2013.
- [17] C. Le, C. Hu, D. English, J. Cannizzaro, Z. Chen, C. Kovach, C. J. Anastasiou, J. Zhao, and K. L. Carder, "Inherent and apparent optical properties of the complex estuarine waters of Tampa Bay: What controls light?" *Estuarine, Coastal Shelf Sci.*, vol. 117, pp. 54–69, Jan. 2013.
- [18] C. Le and C. Hu, "A hybrid approach to estimate chromophoric dissolved organic matter in turbid estuaries from satellite measurements: A case study for Tampa Bay," *Opt. Exp.*, vol. 21, no. 16, pp. 18849–18871, Aug. 2013.
- [19] Z. Lee, K. L. Carder, and R. A. Arnone, "Deriving inherent optical properties from water color: A multiband quasi-analytical algorithm for optically deep waters," *Appl. Opt.*, vol. 41, no. 27, pp. 5755–5772, Sep. 2002.
- [20] C. R. McClain, G. C. Feldman, and S. B. Hooker, "An overview of the SeaWiFS project and strategies for producing a climate research quality global ocean bio-optical time series," *Deep-Sea Research II*, vol. 51, no. 1–3, pp. 5–42, Jan./Feb. 2004.
- [21] F. Mélin, G. Zibordi, and J.-F. Berthon, "Assessment of satellite ocean color products at a coastal site," *Remote Sens. Environ.*, vol. 110, no. 2, pp. 192–215, Sep. 2007.
- [22] A. Morel, D. Antoine, and B. Gentili, "Bidirectional reflectance of oceanic waters: Accounting for Raman emission and varying particle scattering phase function," *Appl. Opt.*, vol. 41, no. 30, pp. 6289–6306, Oct. 2002.
- [23] B. A. Schaeffer, J. D. Hagy, R. N. Conmy, J. C. Lehrter, and R. P. Stumpf, "An approach to developing numeric water quality criteria for coastal waters using the SeaWiFS satellite data record," *Environ. Sci. Technol.*, vol. 46, no. 2, pp. 916–922, Jan. 2012.
- [24] M. Wang, X. Liu, L. Tan, L. Jiang, S. Son, W. Shi, K. Rausch, and K. Voss, "Impacts of VIIRS SDR performance on ocean color products," *J. Geophys.*, vol. 118, no. 18, pp. 10347–10360, Sep. 2013.
- [25] G. Zibordi, J.-F. Berthon, F. Mélin, D. D'Alimonte, and S. Kaitala, "Validation of satellite ocean color primary products at optically complex coastal sites: Northern Adriatic Sea, Northern Baltic Proper and Gulf of Finland," *Remote Sens. Environ.*, vol. 113, no. 12, pp. 2574–2591, Dec. 2009.
- [26] S. Maritorena, O. Hembise Fanton d'Andon, A. Mangin, and D. A. Siegel, "Merged satellite ocean color data products using a bio-optical model: Characteristics, benefits and issues," *Remote Sens. Environ.*, vol. 114, no. 8, pp. 1791–1804, 2010.